High-Resolution Synchrotron Photoemission Studies of the Electronic Structure and Thermal Stability of CH_3- and C_2H_5-Functionalized Si(111) Surfaces

Bengt Jaeckel,[†] Ralf Hunger,*[,†] Lauren J. Webb,[‡] Wolfram Jaegermann,[†] and Nathan S. Lewis*[,‡]

Institute of Materials Science, Technische Universität Darmstadt, Petersenstr. 23, 64287 Darmstadt, Germany, and Beckman Institute and Kavli Nanoscience Institute, Division of Chemistry and Chemical Engineering, 210 Noyes Laboratory, 127-72, California Institute of Technology, Pasadena, California 91125

Received: July 2, 2007; In Final Form: August 20, 2007

The relative coverage, thermal stability, and electronic properties of CH_3- and C_2H_5-functionalized Si(111) surfaces prepared by a two-step chlorination/alkylation procedure have been compared using high-resolution synchrotron photoemission spectroscopy. Whereas the CH_3-terminated Si(111) surface showed only one C 2s peak for the occupied σ orbitals, the C 2s spectra of C_2H_5-terminated Si(111) surfaces showed a symmetric splitting of the occupied σ orbitals, as expected for an ethyl moiety bonded to the surface. The C_2H_5 termination resulted in an unpinning of the Si surface Fermi level, with a band bending of ~0.2 eV, and produced a surface dipole potential step of −0.23(15) eV. The observed close-to-flat-band condition is similar to that of CH_3−Si(111) and is consistent with H termination of the non-alkylated Si atop sites in the two-step chlorination/alkylation process. The C_2H_5-functionalized Si(111) surfaces decomposed at temperatures >300 °C, whereas CH_3−Si(111) surfaces were stable up to at least 440 °C. The data clearly highlight the similarities and identify some significant differences between the behavior of the CH_3- and C_2H_5-functionalized Si(111) surfaces.

I. Introduction

Si(111) surfaces are of interest because they are can be prepared in a chemically and structurally well-defined state by controlled wet chemical etching in $NH_4F(aq)$, which yields a H-terminated Si(111) surface that possesses large terraces on which Si atop atoms are terminated by H atoms oriented normal to the surface plane. Functionalization of the Si(111) surface with alkyl groups has been shown to produce surfaces that are both chemically passivated toward air oxidation and electrically passivated toward surface-derived charge-carrier recombination.[1] Because the distance between Si atop sites on an unreconstructed Si(111) surface is 3.8 Å,[2] methyl groups are the only saturated alkyls that can sterically terminate every atop site on an unreconstructed 1×1 Si(111) surface (Figure 1a).[3−5] The functionalization of H−Si(111) with CH_3− groups, through a two-step chlorination/alkylation process, has been shown, by low-energy electron diffraction (LEED),[6] infrared (IR) absorption spectroscopy,[7] and scanning tunneling microscopy (STM),[5] to produce consistently highly ordered surfaces, with essentially complete (i.e., >90%) termination of surface Si atoms by Si−C bonds.

In contrast, functionalization with C_2H_5− groups can yield only partial termination of the Si(111) surface by Si−C bonds (Figure 1b). X-ray photoelectron spectroscopy (XPS),[8] IR,[7] and STM[9] data have indicated that the remaining Si atop sites on C_2H_5-functionalized Si(111) surfaces prepared by the chlorination/alkylation method are terminated by H atoms, with an estimated Si−C coverage of ~0.8 of a monolayer of Si atop sites on an unreconstructed Si(111) surface. Quantum mechanics

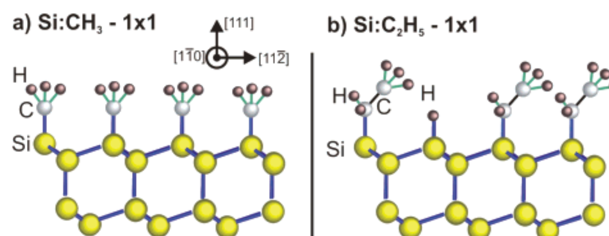

Figure 1. Schematic representation of (a) CH_3- and (b) C_2H_5-functionalized Si(111) surfaces.

calculations are consistent with these coverages for preparation of the ethyl-terminated Si(111) surface through the highly exoergic reaction between a Grignard reagent and the metastable Cl-terminated Si(111) surface.[10] C_2H_5-functionalized Si(111) surfaces also have been shown to be remarkably resistant toward oxidation in air over extended periods of time.[1,11] Hence it is of interest to characterize C_2H_5−Si(111) surfaces spectroscopically to determine the bonding, electronic structure, and thermal stability.

We describe herein synchrotron-based surface-science studies to characterize, by soft X-ray photoelectron spectroscopy (SXPS), the electronic structure of C_2H_5−Si(111) surfaces. In addition, the surface symmetry of C_2H_5−Si(111) surfaces has been analyzed using LEED. The properties of such surfaces have been compared to those of H−Si(111) and CH_3−Si(111) surfaces, both at room temperature and after various high-temperature anneals.

II. Experimental Section

A. Materials. Si samples were n-type, 0.005−0.02 Ω cm resistivity, P-doped, (111) oriented (miscut angle ±0.5°) wafers obtained from ITME (Poland). The resistivity corresponds to a

* To whom correspondence should be addressed. E-mail: hunger@surface.tu-darmstadt.de (R.H.); nslewis@caltech.edu (N.S.L.).
[†] Technische Universität Darmstadt.
[‡] California Institute of Technology.

10.1021/jp0751413 CCC: $37.00 © 2007 American Chemical Society
Published on Web 11/10/2007

dopant concentration of 10^{19} cm^{-3}, which translates into a Fermi level position, E_F, in the band gap (E_g = 1.12 eV) of $E_F - E_{VBM} = 1.04 \pm 0.02$ eV (E_{VBM} is the energy of the top of the valence band) in the bulk of the sample. Prior to use, the wafers were cut into pieces ~1 cm^2 in projected area.

All solvents were used as received. CH_3MgBr and C_2H_5MgBr (~2 M solutions in tetrahydrofuran (THF)) were obtained from Aldrich Chemical Corp. Water having a resistivity of 18 MΩ cm was obtained from a Barnsted Nanopure system.

B. Surface Functionalization. Si surfaces were functionalized by a two-step chlorination/alkylation procedure.[4-6] Briefly, the H-terminated Si(111) surface was first cleaned by rinsing in a flowing stream of H_2O, CH_3OH, acetone, CH_3OH, and H_2O. After the sample was cleaned, it was placed directly in 40% NH_4F(aq) (Transene, Inc.) for 20 min to etch the native oxide layer and to produce a H-terminated Si(111) surface. During the etching process, the wafers were agitated occasionally to remove the bubbles that formed on the surface. After removal from the etching solution, the sample was rinsed thoroughly with H_2O and dried under a stream of N_2(g).

For further chemical functionalization, the sample was then placed into the entry chamber of a N_2(g)-purged glovebox. The H-terminated Si(111) surface was then exposed to a saturated solution of PCl_5 (99.998%, Alfa Aesar) in chlorobenzene, to which a few grains of benzoyl peroxide had been added. The reaction solution was heated to 90−100 °C for 45 min. The sample was then removed from the reaction solution, rinsed with THF and then with CH_3OH, and dried with a stream of N_2(g).

For alkylation, the Cl-terminated Si(111) sample was immersed in a solution of C_2H_5MgBr in THF (Aldrich). Excess THF was added to the reaction solution to allow for solvent loss, and the solution was heated at 70−80 °C for 5 h. The sample was then removed from the solution, rinsed with copious amounts of THF (first) and CH_3OH, immersed in CH_3OH, and removed from the N_2-purged glovebox. The sample was sonicated for 5 min in CH_3OH and in CH_3CN for a further 5 min and then dried under a stream of N_2(g). Sonication was required to completely remove adsorbed Mg salts from the sample surface. The H−Si(111) and C_2H_5-functionalized Si-(111) samples were then sealed under N_2(g) and transported from Pasadena, CA, to the BESSY synchrotron facility in Berlin, Germany. Prior to use, samples were stored for approximately two weeks in a glovebox that contained <1 ppm of O_2(g) and H_2O(g). Immediately prior to the synchrotron measurements, samples were mounted onto degassed sample plates and were transferred, through air, into the load lock chamber of the surface-science instrumentation. Prior to SXPS analysis in the "as received" state, the samples were degassed for 1−2 h at 50 °C at a pressure of $<1 \times 10^{-8}$ mbar. Two C_2H_5-functionalized samples were investigated in detail, and they exhibited mutually similar spectral features. The spectroscopic properties of the methyl-functionalized samples investigated in parallel were very similar to those reported earlier.[6]

C. Instrumentation. Data using synchrotron radiation were obtained at the SoLiAS experimental station on a third-generation synchrotron, BESSY II, in Berlin.[12] The undulator beamline U49/2-PGM2 provided photon-excitation energies, E_{ex}, between 85 and 1400 eV. All spectra were acquired in normal emission with a SPECS Phoibos 150 analyzer, with pass energies of 5 or 2 eV. The binding energies for all investigated excitation energies were calibrated to the Fermi edge of a freshly evaporated Ag film. The combined experimental resolution, determined from the broadening of the Fermi edge of a Ag film, was <0.2 eV, including the line width of the excitation energy and the line broadening produced by the electron analyzer. All energies reported in this work are binding energies in eV with respect to the Fermi energy, E_F, except where otherwise noted.

D. Annealing Behavior. The annealing step was performed in a separate preparation chamber, with a direct transfer, under vacuum, of the sample to the analysis chamber. The heating stage was degassed prior to use, to minimize contamination that might result from desorption of impurities during resistive heating. In the process of annealing, the chamber pressure was $<5 \times 10^{-9}$ mbar. The thermal stability of the alkyl-terminated Si(111) surfaces was investigated by annealing the sample in steps, with each annealing temperature maintained for 30 min. The sample temperature was measured using a K-type thermocouple that was affixed to the apparatus at a location close to the sample. In a separate run, to calibrate the sample temperature with respect to the heater temperature, instead of the silicon wafer a second thermocouple was mounted on the apparatus. In each run, after a given anneal, the sample was cooled to room temperature and was investigated using SXPS. After SXPS data collection, the next annealing step, at a higher temperature, was performed with the same sample. This procedure was repeated until the overlayer had obviously decomposed, as indicated by the SXPS data.

E. Data Analysis. The observed kinetic energies were converted to binding energies, and a detailed analysis of the SXPS data was then performed using Wavemetrics Igor Pro software. Emissions were fitted with a least-squares fitting procedure to a combination of Gaussian and Lorentzian functions. The lowest number of reasonable components was used in each fit. The Si 2p emission was fitted with doublets that were constrained to have a spin-orbit splitting of 0.606 eV and an areal branching ratio of 0.52.[6] The Si 2p emission typically exhibited a Gaussian width of 0.38 eV and a Lorentzian broadening of ~0.1 eV. The C 1s emissions of the ethyl-functionalized sample were best fitted with seven peaks, to account for two chemically different carbon species each having two vibrational components (C^1 and C^2)[6] along with a high-energy C 1s emission, ascribable to adventitious oxidized hydrocarbon. The main C 1s emission typically exhibited a Gaussian width of 0.5 eV and a Lorentzian broadening of ~0.1 eV.

Error estimates are given in parentheses for all quantities determined in this study. These estimates are maximum error estimates and for values with dependencies, such as the surface dipole potential, are the sum of the single-value errors. The actual error is therefore likely to be smaller than the reported error.

III. Results

A. Characterization of the C_2H_5-Terminated Si(111) Surface. *1. Wide-Scan SXPS Data.* Figure 2 shows the SXPS-survey spectrum at E_{ex} = 650 eV of a C_2H_5-functionalized Si-(111) surface. As expected, signals were observed for Si 2p, Si 2s, Si LMM, C 1s, and O 1s emissions. The O 1s emission primarily reflects adsorbed contamination, presumably as water, and possibly contains some contribution from oxidized areas of the surface. The observed O 1s intensity represents 0.3 monolayers of O, as calculated from the spectrometer transmission function and the relative photoelectron cross sections of the C 1s and O 1s peaks, by use of the C 1s intensity signal of a different sample (a CH_3-terminated Si(111) surface after being annealed at 440 °C) as an intensity reference for one monolayer of carbon in the form of methyl groups (vide infra). A detailed analysis of the Si 2p emission with E_{ex} = 150 eV (Figure 2,

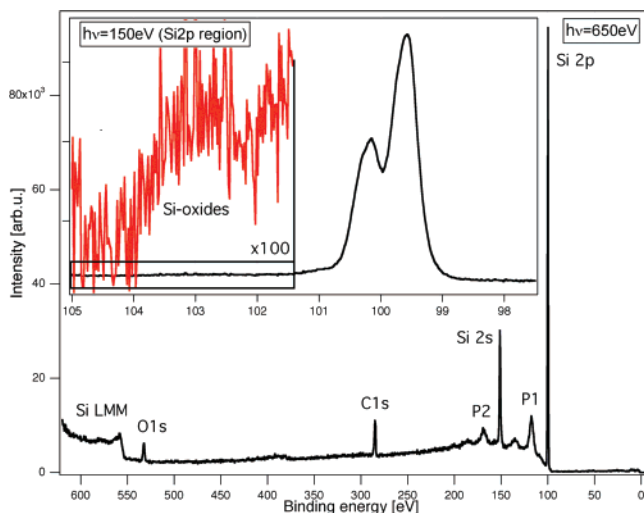

Figure 2. SXPS survey spectrum of a C_2H_5-terminated Si(111) surface excited with a photon energy of 650 eV. The main emission lines are indicated. Peaks labeled P1 and P2 represent well-defined surface plasmon emissions from the Si 2p and Si 2s emissions, respectively. The inset shows a detailed spectrum of the Si 2p emission lines ($E_{ex} = h\nu = 150$ eV) indicating only very small amounts of Si surface oxides (ordinate expanded by a factor of 100).

inset) showed that the overall surface oxidation was less than 5% of a monolayer of Si.

2. Si 2p SXPS Data. Figure 3a displays the SXPS data at various excitation energies for the Si 2p region of the C_2H_5-functionalized Si(111) surface. The Si 2p emission consisted of three components, labeled as (B) for bulk, (C) for carbon-bound, and (H) for hydrogen-bound Si species. The main Si 2p component (B) appeared at 99.58(05) eV. The second component (C) appeared at ~250 meV higher binding energy with respect to the main component (B), and the third component (H) was shifted by ~150 meV to higher binding energies with respect to the main Si 2p emission (B).

The highest surface sensitivity for SXPS of Si in the Si 2p region is obtained at $E_{ex} \sim 150$ eV. The intensities of peaks (C) and (H), assigned to the surface species, decreased consistently in intensity for $E_{ex} > 150$ eV. The (C) component can thus be attributed to Si atoms bonded to carbon atoms through the C_2H_5-surface termination, and the (H) component is assigned to Si−H bonds produced by residual hydrogen termination of the C_2H_5-functionalized Si(111) surface. The energy of the (H) component is comparable to values reported previously for H-terminated Si(111) surfaces.[13,14] At $E_{ex} = 150$ eV, the integrated intensity of the (H) component was 0.34(05) I_0, where I_0 is the integrated intensity of the main emission (B). The (C) component had an integrated area of 0.61(05) I_0. The intensities of the (H) and (C) components relative to the (B) component, along with an escape depth of 3.5 Å for $E_{ex} = 150$ eV, yield a surface coverage of 64 ± 10% of ethyl groups and 36 ± 15% of hydrogen, where a monolayer is defined to be 100% coverage of the atop sites on an unreconstructed Si(111) surface.

All measured values derived from analysis of the Si 2p emission SXPS data are summarized in Table 1. The observed binding energy of the Si 2p bulk signal at 99.58 eV can be used to determine the difference between the Fermi level and the energy of the valence-band maximum. A value of $E_F - E_{VBM} = 0.84(05)$ eV was obtained, assuming a value reported previously for $E_{VBM} - E_{Si2p}$ of 98.74 eV.[15] The data indicate a slight band bending, of ~0.2 eV, on the C_2H_5-functionalized Si(111) surface.

3. C 1s SXPS Data. Figure 3b shows the SXPS data in the C 1s region of the C_2H_5-terminated Si(111) surface. The data were obtained with two excitation energies ($E_{ex} = 330$ eV and $E_{ex} = 650$ eV). The data exhibited three main emissions, with the first two emissions each accompanied by a vibrational excitation signal. In fitting the data, the vibrational excitations were constrained to a 3:2 intensity ratio (Table 2, 0.49:0.33), corresponding to the ratio of C−H bonds in the CH_3− and CH_2− groups of the putative surface-bound $-C_2H_5$ species. A constant binding energy shift with respect to the corresponding main emission, equal in magnitude to the vibrational energy shift observed previously for the CH_3-terminated Si(111) surface, was also used to generate the fits to the data.[6] The spectrum was well fitted with this approach (Figure 3b, Table 2).

The highest surface sensitivity for the C 1s core-level emission was obtained with $E_{ex} \sim 330$ eV. Although both the C atoms in the $-C_2H_5$ group are very close to the surface, if the methyl C atom (i.e., the C atom bonded to three H atoms) is the outermost carbon, it would be expected to exhibit a slightly higher intensity than the second, methylene-type, C atom. This behavior is consistent with the C 1s SXPS data for $E_{ex} = 330$ eV (Figure 3b). The C 1s emission at 284.28(05) eV is therefore assigned to the C atom bonded to Si, denoted as C_{Si}. The binding energy value observed for this emission is similar to the value determined for the C_{Si} 1s emission of the CH_3-terminated Si-(111) surface.[6] The emission at 285.04(05) eV is therefore consistently assigned to the methyl C atom, C_{CH_2} (to denote that the carbon atom of interest, i.e., the H_3C-based methyl carbon, is the carbon atom that is bonded to a $-CH_2-$ group), of the C_2H_5− group. This assignment is in accord with prior literature results for C 1s emissions of methyl groups on surfaces that have been alkylated with long-chain hydrocarbons.[3,8]

Only a small amount of a residual signal, possibly due to adventitious hydrocarbon, was observed in the C 1s region (Figure 3b, third peak: broad emission at 286−287 eV). The emissions associated with the adventitious hydrocarbon generally contain C bonded to H or C, producing a signal at binding energies near 286 eV, and C bonded to O, producing a signal at 287 eV. The observed residual signal is thus consistent with the presence of low levels of such species on the C_2H_5-terminated Si(111) surface. Notably, the levels of adventitious hydrocarbon observed herein are significantly lower than those in other XPS measurements of C_2H_5−Si(111) surfaces, prepared by nominally identical methods.[3] This behavior attests to the lack of extensive adventitious hydrocarbon on the samples in the current vacuum apparatus, and the level was retained even though the samples were shipped to Berlin and were maintained for extended time periods under N_2(g) before being analyzed.

4. C 2s and Valence-Band Emissions of C_2H_5-Terminated Si(111) Surfaces. Figure 4 shows the SXPS data in the valence-band region of CH_3- and C_2H_5-functionalized Si(111) surfaces. As reported previously,[6] the CH_3−Si(111) surface showed a single distinct emission at ~16.4 eV, which can be assigned to the C 2s emission.[16,17] The C_2H_5-functionalized Si(111) surface, in contrast, exhibited a pronounced splitting of the C 2s emission. This splitting is in accord with expectations based on the formation of bonding and antibonding occupied C−C σ-molecular orbitals in the C_2H_5− group (Figure 4). The observed splitting of ±1.73 eV is quite symmetric and consistent, after consideration of a shift of 200 meV for the σ (Si−C)-bond emission relative to that observed for CH_3-terminated Si(111). The observed C 2s splitting of ~3.46(05) eV is in good agreement with the 3.6 eV splitting of the C 2s emission

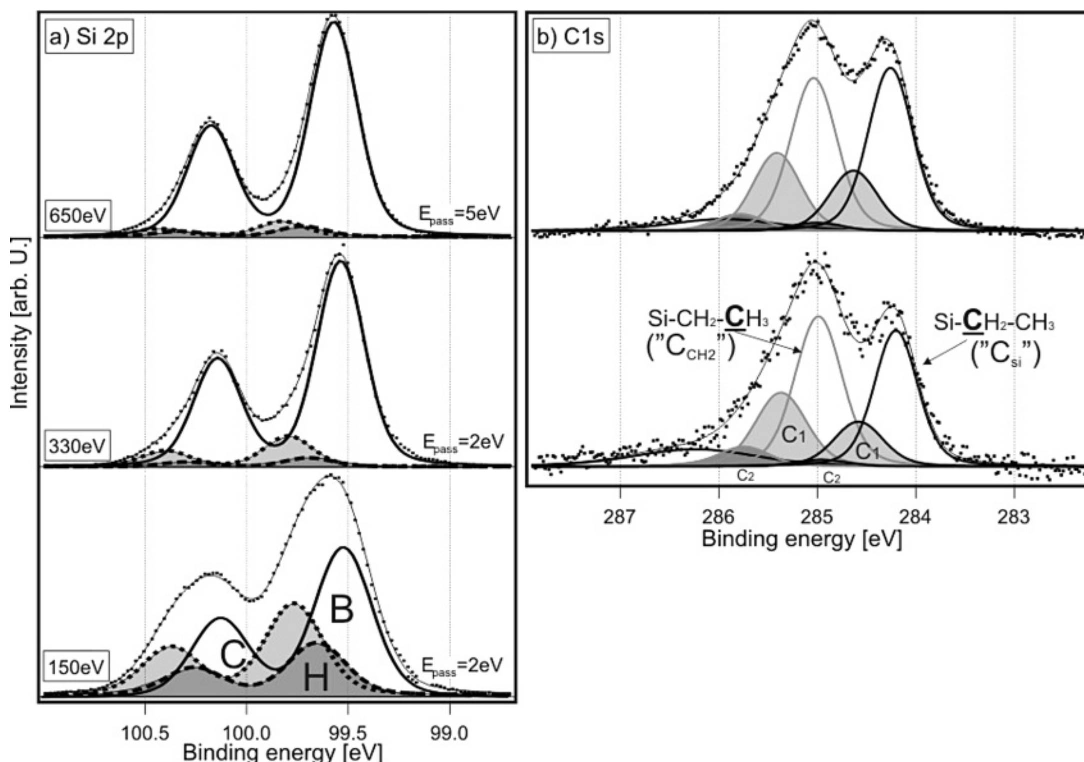

Figure 3. SXPS spectra of (a) the Si 2p emission at photon energies of 150, 330, and 650 eV and (b) the C 1s emission region. The dots represent the raw data after background subtraction, whereas all other lines are results from the fitting procedure.

TABLE 1: Binding Energies and Relative Intensities of the Si 2p Emission for the Investigated C_2H_5-Terminated Si(111) Surface[a]

Si 2p	B = bulk	H = hydrogen	C = C_2H_5
binding energy (eV)	99.58	99.73	99.80
Gaussian width (eV)	0.28	0.28	0.28
relative intensity I/I_0 (150 eV)	1.00	0.34	0.61
I/I_0 (330 eV)	1.00	0.04	0.15
I/I_0 (650 eV)	1.00	0.04	0.07

[a] Binding energies typically had an error of ±0.05 eV, and the relative intensities had an error of ±0.05 I_0.

TABLE 2: Binding Energies of the C_2H_5- Group C 1s Emission Peaks[a]

C 1s	label	binding energy	Δ Vib_1	Δ Vib_2	Int Vib_1	Int Vib_2
Si−**C**H_2−CH_3	C_{Si}	284.28	0.38	0.76	0.33	0.05
Si−CH_2−**C**H_3	C_{CH2}	285.04	0.38	0.76	0.49	0.13

[a] Each component consisted of two vibrational components with a constant binding energy shift, resulting from the C−H-stretch vibrations. Binding energies typically had an error of ±0.05 eV, and the relative intensities had an error of ±0.05 I_0.

observed for gaseous ethane[16] or for the carbon-containing species produced by deposition of diethylsilane on Si(100).[17]

The valence-band maximum was determined as indicated by the straight lines in the upper part of Figure 4a. By this method, a value of $E_F - E_{VBM} = 0.86(05)$ eV was obtained for the C_2H_5-functionalized Si(111) surfaces. As described above, a value of $E_F - E_{VBM} = 0.84(05)$ eV was calculated from the Si 2p core-level emission line. These values thus agree well, within the experimental error.

5. Electron Affinity and Surface Dipole of C_2H_5-Terminated Si(111) Surfaces. The work function, Φ, of the C_2H_5-functionalized Si(111) surface was determined from the secondary-electron onset in spectra obtained with $E_{ex} = 21.2$ eV (HeI), 101, and 650 eV. A value of $\Phi = 4.10(10)$ eV was obtained, which is slightly higher than the value obtained for a CH_3−Si(111) sample having the same dopant concentration.[6] Combining these data with the value of $E_F - E_{VBM} = 0.84(05)$ eV, determined from the Si 2p core-level data, allowed the construction of a band-energy diagram for the C_2H_5-functionalized Si(111) surface (Figure 5). Assuming a bulk electron affinity of 4.05 eV, the data indicate the presence of a surface dipole potential step of −0.23(15) eV. This potential step value is between the values that have been measured for CH_3−Si(111) (−0.37 eV[6]) and H−Si(111) (+0.12 eV[18]) surfaces and is consistent with the formulation of the C_2H_5-functionalized surface as partially Si−C_2H_5 terminated and partially Si−H terminated. The electronic properties of the C_2H_5-functionalized Si(111) surface determined in this work are summarized in the band-energy diagram displayed in Figure 5.

6. Surface Symmetry of C_2H_5-Functionalized Si(111). After the SXPS studies at different excitation energies, the symmetry of the surface was investigated by using low-energy electron diffraction. Figure 6 shows a representative set of LEED patterns observed for the C_2H_5-functionalized Si(111) surface. The pattern obtained at different electron energies clearly showed a 3-fold symmetry, in accord with the expectations for diffraction from the Si atoms of the surface. Neither a surface reconstruction nor a superstructure induced by the C_2H_5- groups was observed. Hence, the diffraction data indicate that a 1 × 1 termination of the surface results from use of the two-step chlorination/alkylation process to introduce the C_2H_5- groups (and H− groups) onto the Si(111) surface.

B. Thermal Stability of CH_3-Terminated Si(111) Surfaces. *1. Si 2p Core-Level Emission.* After CH_3−Si(111) surfaces were annealed at 300 °C, the Si 2p emission shifted to higher binding energies (see Figure 6 “as-received” vs 300 °C). A similar, but smaller, shift was observed after the next annealing step, in which the sample was maintained at 440 °C for 30 min. The shift toward higher binding energies indicates a reduction of the surface band bending. Thus, the flat-band situation was

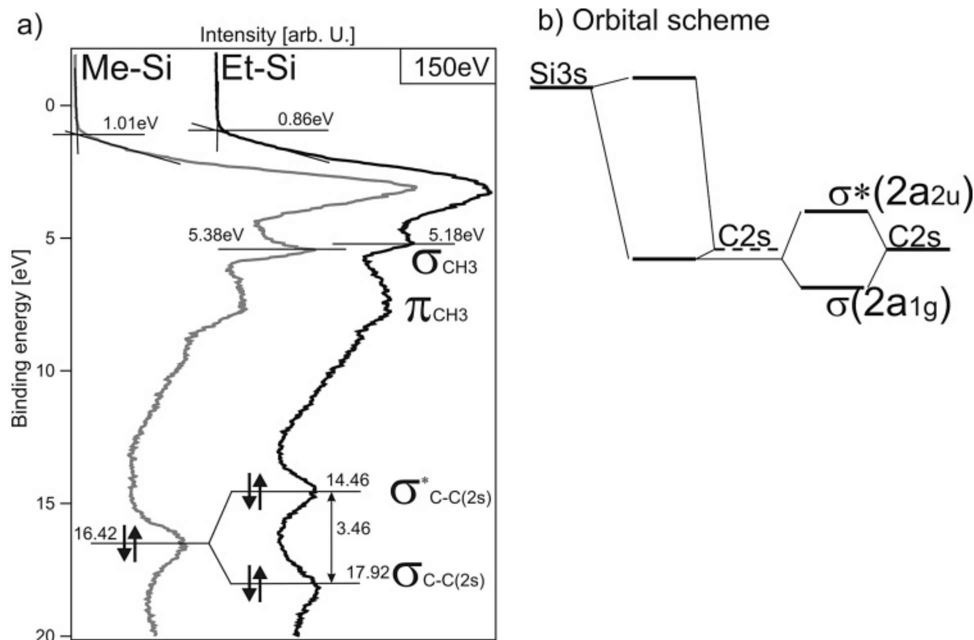

Figure 4. (a) Valence-band region of CH_3- and C_2H_5-functionalized Si(111) surfaces. The σ and π states corresponding to the carbon bonding are indicated in the spectra. (b) A schematic representation of the molecular orbital scheme of the surface.

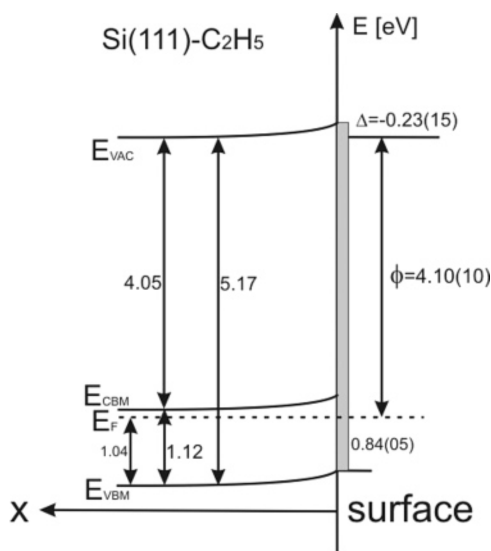

Figure 5. Band-energy diagram of the C_2H_5-functionalized Si(111) surface. Estimated uncertainties are given in parentheses. The positive *x* direction points into the solid from the surface, and the positive energies are closer to the vacuum level, E_{VAC}. The energies of the valence-band maximum, E_{VBM}, the Fermi level, E_F, and the conduction-band minimum are indicated for the bulk and for the surface of the Si.

approached as the contaminants were desorbed. This behavior indicates that the surficial C_xH_y contaminants acted effectively as p-type dopants and produced an adsorbate-induced band bending leading to the observed lower binding energy values for the as-received sample. Removal of such contaminants restored the surface energetics closer to the flat-band conditions and led to a shift to higher binding energies of the Si 2p emission. Other than this shift in the energies of the Si 2p peaks, the CH_3−Si(111) samples exhibited no detectable change in either the intensities or shapes of the emissions in the Si 2p region after either the 300 °C or 440 °C anneals.

The CH_3−Si(111) surface deteriorated considerably, however, after the 530 °C anneal. This deterioration was evidenced by the appearance of a C 1s emission characteristic of silicon carbide at ∼283.5 eV binding energy[19,20] (see Figure 6 lower part), the introduction of a significant asymmetry toward the high binding energy side of the Si 2p emission (E_{ex} = 150 eV, not shown), and a ∼0.2 eV shift of the Si 2p emission toward lower binding energy, consistent with the presence of midgap pinning states on such surfaces.

2. C 1s Core-Level Emission. Figure 6 also shows the SXPS data of the C 1s region of the CH_3−Si(111) surface as a function of annealing temperature. As reported previously, the C 1s region of the as-prepared surface exhibited two prominent emissions, one of which is assigned to C bonded to Si at a binding energy of ∼284.3 eV[6] and the other is assigned to the adventitious hydrocarbon. The lower binding energy emission, characteristic of C bonded to the less electronegative element Si, is not observed for adventitious hydrocarbons on Au (e.g., a calibration sample) and is not present on the non-alkylated, H-terminated Si(111) surfaces (see lowest spectrum in Figure 6 C 1s − Si(111)-H). The higher binding energy C 1s emission also contained a contribution from the vibrational excitation peak that accompanied the 284 eV C_{Si} 1s emission.

Annealing the sample at 330 °C and then at 440 °C produced a decrease in the amplitude of the high binding energy signal ascribed to the adventitious hydrocarbon, while the C_{Si} 1s emission remained unchanged after being annealed at these temperatures. After the 440 °C anneal, the C 1s region was well fitted by a single parent emission at 284.31(05) eV and was accompanied by vibrational loss emissions at 0.38(05) eV and 0.76(05) eV higher in binding energy.[6]

The small shift to higher binding energies of the C 1s emission during the first annealing experiments is consistent with the increase in the binding energy observed for the Si 2p emission (Figure 6), and thus is consequently related to the removal of contamination, with a concomitant reduction in the band bending. Taken together, the Si 2p and C 1s SXPS data therefore are consistent with the hypothesis that the as-prepared CH_3−Si(111) surface consists of a single, Si-bonded methyl surface moiety which, furthermore, is stable up to temperatures of ∼440 °C. After the surface was annealed at 530 °C, the C 1s region showed an additional low binding energy emission, characteristic of Si-carbide (see Figure 6, lower part).

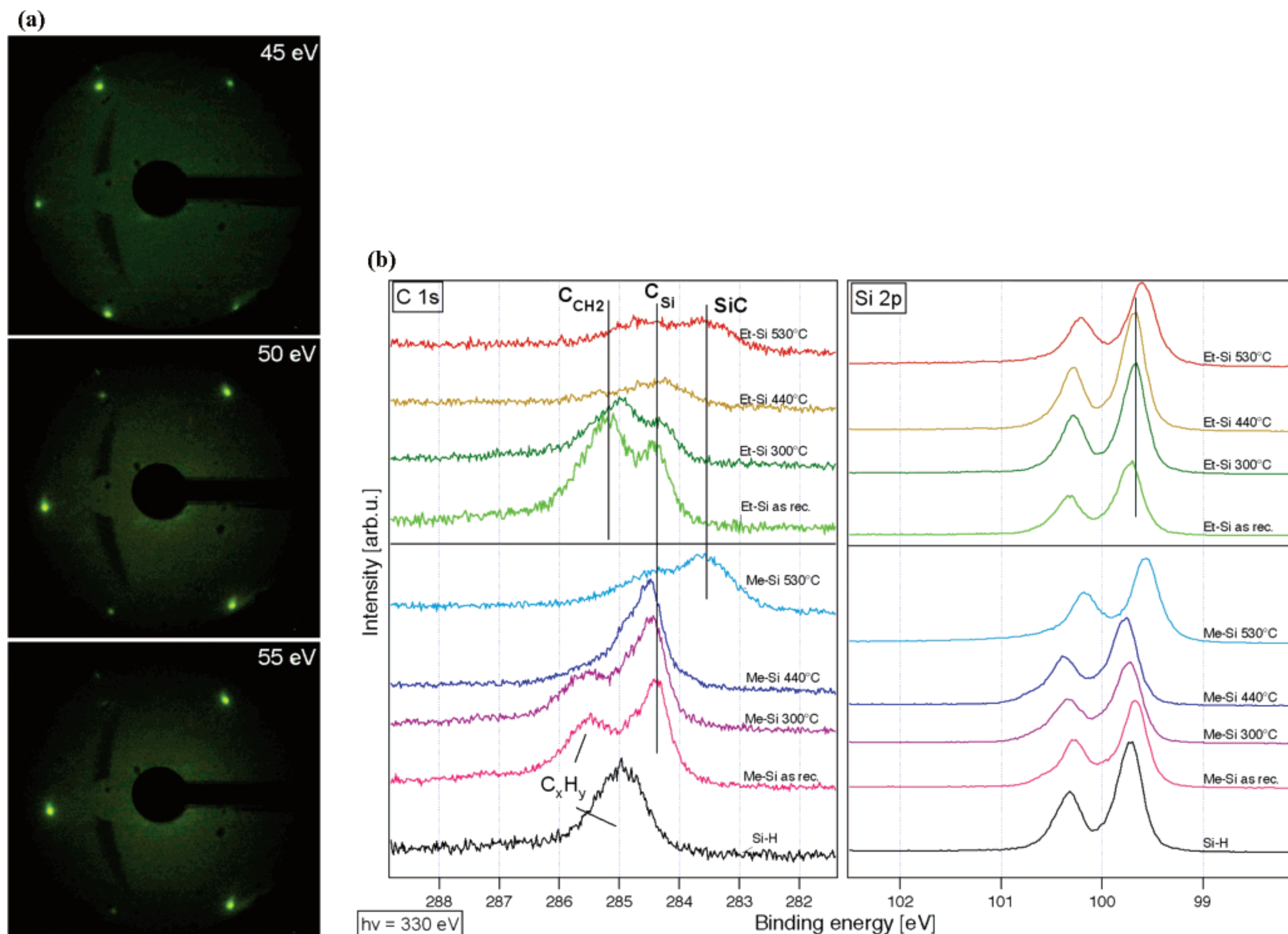

Figure 6. (a) Low-energy electron diffraction patterns of a C_2H_5-functionalized Si(111) surface, recorded at primary-electron energies of 45, 50, and 55 eV. The pattern symmetry is (1 × 1). The width of the spots and the intensity of the diffuse background were comparable to those of hydrogen-terminated or CH_3-functionalized Si(111) surfaces. (b) SXPS data collected before and after several annealing steps to determine the thermal stability of the alkyl-terminated Si(111) surfaces. Methyl-functionalized Si(111) (Me−Si) was more stable (up to at least 440 °C) than the ethyl-functionalized Si(111) (Et−Si). The annealing temperature is indicated in the figure. The reference data for an as-received, hydrogen passivated Si(111) sample are shown at the bottom of the graph.

TABLE 3: Peak-Area Intensities[a] for the Si 2p and C 1s Emissions for H-, CH_3 (Me)-, and C_2H_5 (Et)-Terminated Si(111) Surfaces Determined from Spectra Taken with a Photon Energy of 650 eV[b]

sample	Si 2p (peak area)	C 1s (peak area)	C 1s/Si 2p (relative intensity)	C1 units/ML	C2 units/ML
Si-H	13 985	1204	0.09	0.68	
Me−Si as-received	13 472	2510	0.19	1.48	
Me−Si 300 °C	13 613	2334	0.17	1.36	
Me−Si 440 °C	14 531	1830	0.13	1.00	
Me−Si 530 °C	15 188	1428	0.09	0.75	
Et−Si as-received	14 371	2319	0.16	1.28	0.64
Et−Si 300 °C	15 950	1437	0.09	0.72	0.36
Et−Si 440 °C	16 805	497	0.03	0.23	0.12
Et−Si 530 °C	15 682	1004	0.06	0.51	0.25

[a] All intensity values are normalized to the synchrotron beam current. [b] Details of all calculations are given in the text.

C. Thermal Stability of C_2H_5-Functionalized Si(111) Surfaces. *1. Si 2p Core-Level Emission.* After the first two annealing steps, at 300 °C and 440 °C, little or no change was observed in the Si 2p emission of the C_2H_5-functionalized Si(111) surfaces. The intensity of the Si 2p emission increased somewhat after the 300 °C anneal, presumably due to the partial desorption of ethyl moieties (vide infra). After an annealing step at 530 °C, the Si 2p emission changed in both shape and binding energy. The same shift, to lower binding energies, was also observed on the CH_3-terminated Si(111) surface after a 530 °C anneal. This behavior indicates that the high-temperature thermal decomposition of the functionalized surfaces eventually led to carbide formation, with this process occurring at similar temperatures for the CH_3- and C_2H_5-functionalized Si(111) surfaces.

2. C 1s Core-Level Emission. Annealing the C_2H_5−Si(111) surface at 300 °C produced a decrease in the overall intensity of the C 1s signals, to ~60% of their original amplitude (Table 3 and section IV). The intensity of the silicon-bound C_{Si} component also decreased by ~40%. Furthermore, the characteristic split C 2s emission (cf. Figure 4a) and the σ_{Si-C} bond related valence-band emission feature diminished to ~60% of the intensity observed in the nonannealed state (not shown). In contrast, the general peak shape of the C_2H_5−Si(111) related

C 1s emission, i.e., the relative intensities of the methyl carbon (bonded to a methylene group), C_{CH_2}, and of the silicon-bonded C_{Si} components, as well as the peak positions, remained nearly unchanged as a result of this anneal. The data thus indicate that the first annealing step, at 300 °C, led to the desorption of ~40% of the initially present ethyl moieties.

After the surface was annealed at 440 °C, the high binding energy component of the C 1s signal, i.e., the signal arising from the carbon bonded to a methylene group, C_{CH_2}, almost completely disappeared and the overall C 1s emission shape closely resembled that obtained for the CH_3−Si(111) surface. Thus, after the anneal at 440 °C, all of the initially present ethyl groups either desorbed or decomposed.

The next annealing step, at 530 °C, produced a new emission at significantly lower binding energy, characteristic of carbidic species.[19,20] The overall intensity of the C 1s emission increased after the 530 °C annealing step, presumably due to an insufficient outgassing of the heating stage prior to the experiment. The shape of the C 1s emission after the 530 °C anneal was similar to the shape of the C 1s signal observed for the CH_3−Si(111) surface after a 530 °C anneal, indicating that a similar decomposition reaction product formed at this temperature in both cases.

IV. Discussion

A. Surface Coverage of Alkyls on the Ethyl-Modified Si(111) Surface. Theoretical studies of Si alkylation by the two-step chlorination/alkylation pathway have shown that methyl groups can sterically cover every atop site on an unreconstructured Si(111) surface.[10] This conclusion is in good agreement with experimental data for CH_3−Si(111) surfaces made by the two-step chlorination/alkylation process.[4,5,7] Theoretical studies have also shown that long-chain alkyls will have significant strain at coverages >50% of a monolayer[10] but ethyl overlayers can pack with very small strain for coverages up to at least 66% of a monolayer.[10] This analysis is consistent with prior results indicative of relatively high coverages of ethyl groups formed with the two-step chlorination/alkylation method on Si(111), as measured by the ratio of the low binding energy C_{Si} 1s signal relative to the Si 2p signal intensity for methyl- vs ethyl-terminated Si(111) surfaces.[8] Lower coverages were observed for longer chain alkyls, especially for sterically hindered secondary and tertiary alkyl groups.[8] In contrast, XPS analysis of the absolute signal intensity of the C_{Si} 1s peak for H−Si(111) alkylated by anodic oxidation in the presence of Grignard reagents has yielded C_{Si} 1s signals consistent with a coverage of methyl groups on the order of a monolayer or fraction of a monolayer, with the C_{Si} 1s intensity reported to be twice as large for methyl termination as that for surfaces derivatized with longer alkyl chains.[21] The structures of alkylated Si(111) surfaces have also been investigated theoretically from different perspectives, with computational studies focusing on long-chain alkyl groups, such as octyl or octadecyl groups.[22−25] In some cases, 50% coverage was assumed to be the highest packing available for such alkyl groups, and the minimum energy structure was calculated at this coverage level.[22] In other calculations, the energy per chain for octyl or octadecyl groups attached to the surface was calculated to be minimal at 40−60% alkylation of the unreconstructed Si(111) atop sites, and the minimum energy structures were calculated at the coverage that produced the minimum energy per chain.[24] For these dynamics simulations with long-chain alkyl monolayers, the van der Waals interactions of the chain tails will dominate the packing interactions. The calculated coverage that minimizes the energy per chain would predict the experimentally observed coverage only if the strain energy were the only consideration. However, the free energy change of the reaction must control the final surface coverage, and a sufficiently negative (or positive) free energy change per site reacted can cause the free energy minimum to be different from the strain energy minimum. For surfaces prepared by the chlorination/alkylation method, which has a large free energy change that favors the products relative to the reactants, higher coverages and structures with significant bond strain should be possible thermodynamically, especially for functionalization reactions with very short-chain alkyl groups.[10]

The line shape deconvolution of the Si 2p and the C 1s SXPS emissions of C_2H_5-modified Si(111) surfaces indicates that the two-step chlorination/alkylation process yields a surface in which the SXPS detectable Si atop sites are terminated primarily by Si−C_2H_5 and Si−H bonding. This behavior is also consistent with the lack of significant SXPS-detectable silicon oxide formation on such surfaces, in accord with conclusions from prior XPS, STM, and IR data on such surfaces.[4−7]

Several different approaches can be used to estimate the relative coverages of silicon surface species bonded to hydrogen and ethyl groups from the SXPS data. The relative intensities in the Si 2p region of the peaks labeled B, H, and C in Figure 3a (C/B = 0. 61; H/B = 0.34) collected with E_{ex} = 150 eV are indicative of a surface coverage of 64 ± 10% of ethyl groups on C_2H_5-terminated Si(111) surfaces, with the remaining 36 ± 15% of the SXPS detectable, nonbulk surface Si atoms being terminated with hydrogen.

In a second approach, the relative coverage of all SXPS observable alkyl carbons was evaluated for the CH_3- and C_2H_5-functionalized Si(111) surfaces. In this approach, the total peak areas of the Si 2p and C 1s emissions, including the surface components in the Si 2p region and the vibrational satellites in the C 1s region, were compared for each of the as-received and thermally annealed functionalized Si surfaces. The integrated areas of the Si 2p and C 1s peaks, after background subtraction for the various CH_3- and C_2H_5-terminated Si(111) surfaces, are given in the second ("Si 2p") and third columns ("C 1s") of Table 3 along with the intensity ratio C 1s/Si 2p in the column labeled "C/Si".

Use of this approach requires that all of the analyzed C 1s signal intensity arises from covalently bonded species alkylating the Si surface sites as opposed to arising from adventitious, adsorbed hydrocarbons. The approach also requires a reference surface having a known coverage of alkyl groups. As determined previously for the CH_3-termination layer,[6] the C 1s emission of methyl-terminated Si(111) exhibits a main emission and two vibrational satellites. After desorption of adventitious hydrocarbons during the anneal at 440 °C, the shapes of the emissions (Figure 6) were indicative of an ideally methyl-terminated Si(111) surface. This sample was therefore assumed to have a monolayer coverage of CH_3− groups on Si(111), and the values of the total C 1s and Si 2p peaks on this surface were used as the reference surface values. The higher relative values of the as-received methylated surface in comparison to those of the annealed samples were then consistently assumed to result from adventitious hydrocarbon contamination, which was assumed to be completely desorbed at 440 °C, consistent with the observed SXPS data.

The relative coverage of alkyl carbons on the C_2H_5-functionalized surfaces was then evaluated with respect to the alkyl carbons present on the reference CH_3−Si(111) surface. The integrated C 1s peak area of various C_2H_5-functionalized

TABLE 4: Peak-Area Intensities for the Si 2p and C 1s Emissions for H-, CH_3 (Me)-, and C_2H_5 (Et)-Terminated Si(111) Surfaces Determined from Spectra Taken with a Photon Energy of 330 eV[a]

sample	Si 2p (peak area)	C 1s (peak area)	C 1s/Si 2p (relative intensity)	C1 units/ML	C2 units/ML
Si−H	7298	1220	0.17	0.83	
Me-Si as rec.	5998	1849	0.31	1.54	
Me−Si 300 °C	6036	1904	0.32	1.57	
Me−Si 440 °C	6439	1293	0.20	1.00	
Me−Si 530 °C	6877	1247	0.18	0.90	
Et−Si as rec.	5869	2288	0.39	1.94	0.97
Et−Si 300 °C	6966	1330	0.19	0.95	0.48
Et−Si 440 °C	7654	661	0.09	0.43	0.22
Et−Si 530 °C	6676	1005	0.15	0.75	0.37

[a] A comparison with Table 3 displays the significant differences in relative coverages deduced from data analysis at the different excitation energies.

surfaces, relative to the C 1s peak area of the reference CH_3−Si(111) surface and normalized by the total Si 2p area for each surface, is indicated in the fifth ("C1 units") column of Table 3. The C_2H_5-functionalized Si(111) surface has, however, two nonequivalent C atoms in the C_2H_5-terminated layer. The C 1s deconvolution in Figure 3a indicates that at $E_{ex} = 650$ eV, both C atoms, including their vibrational satellites, contribute approximately equivalently to the C 1s intensity. The coverage in terms of total alkyl carbons deduced from the total observed C 1s area on the C_2H_5-terminated Si(111) surface must therefore be divided by 2 to yield the derived coverage of ethyl groups. This value is displayed in column 6 in Table 3 ("C2 units"). Thus, the relative coverage of C_2H_5− groups on Si(111) for the as-received sample calculated from this method is ~64% of the coverage of methyl groups on the reference CH_3−Si(111) surface ($E_{ex} = 650$ eV). This result is in excellent agreement with the coverage of carbon-bonded Si atoms relative to total Si atop sites determined from the deconvolution of the $E_{ex} = 150$ eV Si 2p SXPS emission data. An analogous analysis, however, performed by using the C1s and Si 2p SXPS data obtained with $E_{ex} = 330$ eV, indicates a relative coverage of C_2H_5− groups on the as-received C_2H_5-functionalized Si(111) sample that is 97% of the coverage of methyl groups on the reference CH_3−Si(111) surface (Table 4). Of course, the entries for the highest temperatures in column 6 of Table 3 are only arithmetical values, because the XPS data indicated that little or no C_2H_5− functionality existed on the surface after anneals at these temperatures.

A third approach relies on the uniqueness of the low binding energy C_{Si} 1s signal as diagnostic of C bonded to Si. This approach does not require the assumption that all of the observed C 1s signal is due to covalently bonded alkyl species, because the low binding energy C 1s signal is unique to carbon bonded to the more electropositive element Si. The ratio of the C_{Si} 1s peak intensity to the Si bulk (B) peak intensity was therefore calculated for all of the surfaces of interest. For CH_3−Si(111) surfaces, the C_{Si}/Si 2p (B) area ratio was essentially constant for samples annealed at ≤440 °C. By use of this approach, for data obtained with $E_{ex} = 330$ eV, the as-received C_2H_5-functionalized Si(111) samples exhibited a C_{Si}/Si 2p (B) area ratio that was 94% of that of the CH_3−Si(111) surface. If the bulk and H-terminated (B and H) Si 2p peaks were combined into one component for the C_2H_5-functionalized Si(111) surface, the ratio decreased only slightly, to 86% of the CH_3−Si(111) surface. Hence, the coverage of carbon bonded to Si atop sites on the as-received C_2H_5−Si(111) surface is calculated from this approach to be 80−90% of that on the as-received, or 440 °C annealed, CH_3−Si(111) surface. This analysis is consistent with the intensity data ratios of the C 1s to Si 2p peaks also obtained with $E_{ex} = 330$ eV. Additionally, the value is in agreement with XPS data obtained independently, on independently prepared samples, by using 1486.6 eV Al Kα excitation, which yielded a coverage of carbon bonded to Si sites on C_2H_5-functionalized Si(111) surfaces of 80−90% of that on CH_3-terminated Si(111) surfaces.[8] However, the use of this same C_{Si} 1s to Si 2p analysis method on the data obtained with $E_{ex} = 650$ eV indicates a coverage of carbon bonded to Si sites on atop sites on the as-received C_2H_5−Si(111) surface that is 67% of that on the as-received, or 440 °C annealed, CH_3−Si(111) surface. This value is consistent with the value obtained by use of the integrated C 1s to Si 2p peak intensities at this same photoelectron excitation energy.

In a fourth approach, the absolute intensity of the C 2s emissions at 15−18 eV (cf. Figure 4) was evaluated for the C_2H_5- and CH_3-functionalized Si(111) surfaces. At $E_{ex} = 150$ eV, the integrated intensity of the high binding energy C 2s emissions at 13.8 eV on the C_2H_5-functionalized Si(111) surfaces was 64 ± 15% of the intensity of the C 2s emission observed on the 440 °C annealed CH_3-terminated Si(111) surface.

Each method of determining the coverage involves some assumptions and has associated errors. The C_{Si}/Si 2p ratiometric method may be affected by photoelectron diffraction and requires assumptions regarding the coverage of a reference sample. The ratio of peaks C, B, and H in the Si 2p region does not depend on a reference sample but relies on the assumption that the components C and H represent one full monolayer coverage. The accuracy of the peak ratio C/H is limited by ambiguities in the curve fitting, where the three components C, H, and B are located within an energy window of 250 meV, which is on the order of the peak width of 280 meV of the individual components. The integrated C 1s area ratio method requires use of a reference sample and additionally assumes that all of the detected carbon on the CH_3- and C_2H_5-functionalized Si(111) surfaces only arise from CH_3− or C_2H_5− groups, respectively. However, the analysis using this approach yields values that are internally consistent with those obtained from the analysis of the relative areas of the deconvoluted peaks in the Si 2p region of the spectrum. More importantly, the data obtained with $E_{ex} = 650$ eV are internally mutually consistent at an indicated C_2H_5− vs CH_3− relative coverage of 67%, whereas the data obtained with $E_{ex} = 330$ eV are internally mutually consistent with an indicated C_2H_5− vs CH_3− relative coverage of 80−90%. In addition, the former values are consistent with the analysis of the integrated C 2s intensity at $E_{ex} = 150$ eV for the C_2H_5- vs CH_3-functionalized Si(111) surfaces. Photoelectron diffraction effects must be considered carefully in analysis of the SXPS and XPS data for such surfaces. Such effects can be especially important for the low photon-excitation energies used in SXPS,[3] with significant

contributions to the observed intensity from back-scattered photoelectrons, and additionally can be manifest for the high photon-excitation energies used in laboratory XPS experiments, which may contain significant contributions from forward-scattered photoelectrons.[26] For the SXPS data, photoelectron diffraction effects are expected to be less important for the higher energy $E_{ex} = 650$ eV excitation, where less than 5% error is estimated to arise from such effects. This suggests that the lower coverage values deduced from the analysis with $E_{ex} = 650$ eV photoelectron excitation energy are probably closer approximations to the true relative coverage of alkyl groups on the C_2H_5- vs CH_3-functionalized surfaces. In all cases, the analysis is generally indicative of a rather high coverage of alkyls on ethyl-functionalized Si surfaces, consistent with other STM and IR studies[7,9] as well as with theoretical predictions of the possible saturation coverage of alkyls that can be accommodated, in principle, on Si(111) surfaces due to the highly exoergic reaction between the Grignard reagents and Cl-terminated Si surfaces.[10]

B. Thermal Stability Limits of Methyl- and Ethyl-Modified Si(111) Surfaces. The annealing experiments have revealed the thermal stability limits of the CH_3- and C_2H_5-functionalized Si(111) surfaces. The evolution of the Si 2p emission suggests that both surfaces have a stability limit of ≤440 °C. For higher annealing temperatures, the spectral features of silicon carbide clearly appeared.

For CH_3−Si(111) surfaces, the C 1s emission indicated a thermal stability limit of ∼440 °C. The CH_3-passivation layer therefore exhibits a thermal stability range similar to that of hydrogen termination, Si(111)−H, for which the onset of (monohydride) desorption has been reported[27] to occur at ∼480 °C for very flat surfaces with a low density of steps, comparable to the samples used in this study. A decreased stability limit was observed for Si(111)−H surfaces when rough surfaces were studied. An inorganic surface termination layer with an even higher thermal stability limit is the GaSe half-sheet termination, which is stable to ∼550 °C.[28−30]

Earlier studies of the thermal decomposition of longer chain alkylated surfaces have reported stability limits of ∼200 °C for surfaces such as ethyl-functionalized Si(111).[31] Thermally induced disorder in a monolayer of octadecyl-terminated Si(111) prepared by the thermal addition of octadecene to H−Si(111) surfaces has been observed at <100 °C, with irreversible conformational disorder introduced at 170 °C and desorption inferred by IR spectroscopy of the remaining surface alkyls at 220 °C.[32] The methyl-termination thus exhibits the greatest thermal stability of the alkyl-terminated Si(111) systems reported to date.

The thermal stability limit of ethyl-functionalized Si(111) was <300 °C, because desorption of ethyl units was apparent even in the first annealing step at 300 °C. At this temperature, the shape of the C 1s emission did not change, but the C 1s signal intensity decreased by ∼40%. The nearly constant binding energy of the Si 2p emission (Figure 6) is consistent with the hypothesis that, during this anneal, Si−H bonds were formed at the sites that had lost Si−C termination. The production of unsaturated dangling bonds would, in contrast, be expected to result in increased band bending and in Fermi level pinning near midgap. The conclusions from the present SXPS study are in accord with previous investigations of the thermal stability of ethylated Si(111) by in situ infrared spectroscopy,[31] which observed a decrease in ethyl coverage by 40%, including the hydrogen termination of the created surface sites, upon annealing ethylated Si(111) at 300 °C.

A mechanism consistent with these observations involves Si−C bond cleavage according to β-hydride elimination, accompanied by the formation of ethene.

$$\equiv Si-CH_2-CH_3 \rightarrow \equiv Si-H + H_2C{=}CH_2\ (g) \quad (1)$$

This mechanism is consistent with the β-hydride elimination reaction observed at similar temperatures (reported as 650 K) for the decomposition of octadecyl-terminated Si(111) surfaces prepared by the thermal addition of octadecene to H−Si(111) surfaces.[33] Since the surface site density of Si(111) is 7.8×10^{14} cm^{-2}, the decomposition of 0.5 monolayers of Si bonded as Si−C_2H_5 would, for example, produce 6.5×10^{-10} mol cm^{-2} of gaseous ethylene.

The C_2H_5-functionalized Si(111) surface when annealed at 440 °C exhibited a pronounced change in the shape of the C 1s emission. The resulting emission was similar to the emission of the CH_3-terminated Si(111) surface, but with a reduced intensity. The high binding energy component assigned to the carbon bonded to a methylene unit, C_{CH_2}, disappeared almost completely after this anneal. Because the high binding energy emission is related to the methyl C atom in the C_2H_5− group, the data suggest a significant contribution from cleavage of the C−C bond during the decomposition process in this annealing step. The C_{Si} 1s intensity indicated a relative coverage of ∼0.23 ML of $-CH_3$ units after this annealing step. The data are therefore consistent with a significant contribution to desorption from a second thermal decomposition process:

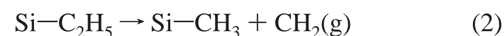

$$Si-C_2H_5 \rightarrow Si-CH_3 + CH_2(g) \quad (2)$$

This process is analogous to the minority reaction proposed from IR spectroscopy for the decomposition at 200−350 °C of decyl-terminated Si(111) surfaces, prepared by the thermal addition of decene to H−Si(111) catalyzed by ethylaluminum chloride.[34] Of course, the relative proportions of decomposition processes (eqs 1 and 2) observed in this work are not fundamental constants but instead reflect the branching pathways observed for the specific time and temperature history of the samples investigated. For example, the minor contribution of the process of eq 2 observed in the decomposition of decyl-terminated Si(111) surfaces may well reflect the different temperature steps and rate of temperature rise (i.e., 50 °C steps at 15 min each) used in that study;[34] a slower rate of temperature rise would favor desorption proceeding primarily through the process exhibiting the lowest activation barrier, whereas a faster rate of temperature rise could lead to several desorption paths taking place in parallel. Subsequent to the process of eq 2, as a gas-phase or a surface-phase reaction, two CH_2− groups could subsequently combine to form ethene, C_2H_4.

During the last annealing step, at 530 °C, the same low binding energy component was visible in the C 1s spectra of C_2H_5-functionalized Si(111) as was observed in the spectra of the CH_3−Si(111) surface. The temperature of this annealing step was, however, well above the known stability limit of Si−H bonds. Thus, C atoms, bonded to at least two Si atoms, are the only stable species at this temperature. These C atoms would lead to the observed low binding energy component in the C 1s emission as well as to the observed shift in Si 2p binding energy to lower values, corresponding to binding energies typically observed for Fermi level pinned Si-surfaces.

V. Summary

Synchrotron-induced photoelectron spectroscopy has been used to determine the chemical bonding and electronic structure of C_2H_5-functionalized Si(111) surfaces as well as the thermal stability of C_2H_5-Si(111) and CH_3-Si(111) surfaces prepared by a two-step chlorination/alkylation method. Attachment of a surface-bound C_2H_5- group produced a core-level shift of 250(50) meV in the Si 2p emission derived from the Si surface atoms. The C 1s emission consisted of two main components, C_{Si} and C_{CH_2}, which corresponded to emissions from the silicon-bound methylene groups (C_{Si}) and from the topmost aliphatic, methylene-bonded methyl groups (C_{CH_2}), respectively. Due to the bonding with the more electropositive Si, C_{Si} was shifted with respect to C_{CH_2} by $-0.76(05)$ eV. The ethyl-related emissions C_{Si} and C_{CH_2} each exhibited two vibrational satellites, derived from the excitation of C$-$H stretch vibrations. These peaks were shifted by $\Delta E_{vib} = +0.38(05)$ and $+0.76(05)$ eV, respectively, from the main C 1s signal for each type of carbon atom. The ratio of the vibrational satellite intensities fitted well to the number of attached H atoms on each carbon ($-CH_2/-CH_3 = 2:3$). The direct covalent bonding of ethyl groups to silicon was further evidenced by a characteristic valence state emission from the silicon$-$carbon bond orbital, $\sigma_{Si-C(2p)}$, at a binding energy of 4.32(10) eV with respect to the valence-band maximum. The C 2s orbital was split into bonding and antibonding contributions of the adsorbed ethyl moiety, with an energy separation of 3.46(05) eV and with the $\sigma^*_{C-C(2s)}$ orbital energy being 13.60(10) eV below the valence-band maximum. Analysis of the Si 2p peak intensities of the C_2H_5-Si(111) surface indicated that 65$-$95% of the surface was terminated by C_2H_5- groups, with the remaining portion of SXPS detectable sites being terminated by hydrogen atoms.

The thermal stability of the CH_3- and C_2H_5-functionalized Si(111) surfaces was investigated by a stepwise annealing procedure. A thermal stability limit of ~440 °C was observed for the CH_3-Si(111) surface, whereas the C_2H_5-functionalized Si(111) surface was stable only to $<$300 °C. The data are consistent with two main decomposition reactions for the C_2H_5-termination layer. During the decomposition reaction at temperatures $<$440 °C, the data are consistent with a primary decomposition pathway involving the formation of gaseous C_2H_4, with the additional H atoms forming H$-$Si(111) bonds. When annealed at temperatures $>$440 °C, surface carbidization was observed, as indicated by a shift in binding energy in the Si 2p spectra and a low binding energy component in the C 1s emission. The data indicate that CH_3-termination provides a passivated, chemically inert surface for temperatures up to 440 °C.

Acknowledgment. We gratefully acknowledge the National Science Foundation, Grant No. CHE-0604894, for support of this work (N.S.L. and L.J.W.) and for providing a graduate research fellowship to L.J.W. W.J. acknowledges the traveling support of the Deutsche Forschungsgemeinschaft, DFG Grant No. JA 85910-1. The BMBF is acknowledged for support for setting up and running SoLiAS at BESSY (Contracts 05 KS1RD1/0 and 05 KS4RD1/0, R.H. and W.J.) and for travel grants (05 ES3XBA/5). This work was also supported by the European Network of Excellence FAME, WP6.

References and Notes

(1) Royea, W. J.; Juang, A.; Lewis, N. S. *Appl. Phys. Lett.* **2000**, *77*, 1988−1990.
(2) Lifshits, V. G.; Saranin, A. A.; Zotov, A. V. *Surface Phases on Silicon*: *Preparation, Structures, and Properties;* John Wiley & Sons: New York, 1994.
(3) Terry, J.; Linford, M. R.; Wigren, C.; Cao, R. Y.; Pianetta, P.; Chidsey, C. E. D. *J. Appl. Phys.* **1999**, *85*, 213−221.
(4) Webb, L. J.; Nemanick, E. J.; Biteen, J. S.; Knapp, D. W.; Michalak, D. J.; Traub, M. C.; Chan, A. S. Y.; Brunschwig, B. S.; Lewis, N. S. *J. Phys. Chem. B* **2005**, *109*, 3930−3937.
(5) Yu, H. B.; Webb, L. J.; Ries, R. S.; Solares, S. D.; Goddard, W. A.; Heath, J. R.; Lewis, N. S. *J. Phys. Chem. B* **2005**, *109*, 671−674.
(6) Hunger, R.; Fritsche, R.; Jaeckel, B.; Jaegermann, W.; Webb, L. J.; Lewis, N. S. *Phys. Rev. B* **2005**, *72*, Art. 045317.
(7) Webb, L. J.; Rivillon, S.; Michalak, D. J.; Chabal, Y. J.; Lewis, N. S. *J. Phys. Chem. B* **2006**, *110*, 7349−7356.
(8) Nemanick, E. J.; Hurley, P. T.; Brunschwig, B. S.; Lewis, N. S. *J. Phys. Chem. B* **2006**, *110*, 14800−14808.
(9) Yu, H. B.; Webb, L. J.; Solares, S. D.; Cao, P. G.; Goddard, W. A.; Heath, J. R.; Lewis, N. S. *J. Phys. Chem. B* **2006**, *110*, 23898−23903.
(10) Nemanick, E. J.; Solares, S. D.; Goddard, W. A.; Lewis, N. S. *J. Phys. Chem. B* **2006**, *110*, 14842−14848.
(11) Webb, L. J.; Lewis, N. S. *J. Phys. Chem. B* **2003**, *107*, 5404−5412.
(12) Mayer, T.; Lebedev, M.; Hunger, R.; Jaegermann, W. *Appl. Surf. Sci.* **2005**, *252*, 31−42.
(13) Grupp, C.; Taleb-Ibrahimi, A. *J. Electron Spectrosc. Relat. Phenom.* **1999**, *103*, 309−313.
(14) Karlsson, C. J.; Owman, F.; Landemark, E.; Chao, Y. C.; Martensson, P.; Uhrberg, R. I. G. *Phys. Rev. Lett.* **1994**, *72*, 4145−4148.
(15) Himpsel, F. J.; Hollinger, G.; Pollak, R. A. *Phys. Rev. B* **1983**, *28*, 7014−7018.
(16) Hamrin, K.; Johansson, G.; Gelius, U.; Fahlman, A.; Nordlin, C.; Siegbahn, K. *Chem. Phys. Lett.* **1968**, *1*, 613−615.
(17) Lapianosmith, D. A.; Himpsel, F. J.; Terminello, L. J. *J. Appl. Phys.* **1993**, *74*, 5842−5849.
(18) Hunger, R.; Pettenkofer, C.; Scheer, R. *J. Appl. Phys.* **2002**, *91*, 6560−6570.
(19) Contarini, S.; Howlett, S. P.; Rizzo, C.; Deangelis, B. A. *Appl. Surf. Sci.* **1991**, *51*, 177−183.
(20) Muehlhoff, L.; Choyke, W. J.; Bozack, M. J.; Yates, J. T. *J. Appl. Phys.* **1986**, *60*, 2842−2853.
(21) Fellah, S.; Teyssot, A.; Ozanam, F.; Chazalviel, J.-N.; Vigneron, J.; Etcheberry, A. *Langmuir* **2002**, *18*, 5851−5860.
(22) Sieval, A. B.; van der Hout, B.; Zuilhof, H.; Sudholter, E. J. R. *Langmuir* **2000**, *16*, 2987−2990.
(23) Sieval, A. B.; van der Hout, B.; Zuilhof, H.; Sudholter, E. J. R. *Langmuir* **2001**, *17*, 2172−2181.
(24) Yuan, S.-L.; Cai, Z.-T.; Jiang, Y.-S. *New J. Chem.* **2003**, *27*, 626−633.
(25) Zhang, L.; Wesley, K.; Jiang, S. *Langmuir* **2001**, *17*, 6275−6281.
(26) Wallart, X.; de Villeneuve, C. H.; Allongue, P. *J. Am. Chem. Soc.* **2005**, *127*, 7871−7878.
(27) Pietsch, G. J.; Kohler, U.; Henzler, M. *J. Vac. Sci. Technol., B* **1994**, *12*, 78−87.
(28) Amokrane, A.; Sebenne, C. A.; Cricenti, A.; Ottaviani, C.; Proix, F.; Eddrief, M. *Appl. Surf. Sci.* **1998**, *123*, 619−625.
(29) Jedrecy, N.; Pinchaux, R.; Eddrief, M. *Physica B* **1998**, *248*, 67−73.
(30) Meng, S.; Schroeder, B. R.; Olmstead, M. A. *Phys. Rev. B* **2000**, *61*, 7215−7218.
(31) Faucheux, A.; Yang, F.; Allongue, P.; De Villeneuve, C. H.; Ozanam, F.; Chazalviel, J. N. *Appl. Phys. Lett.* **2006**, *88*, 193123−193125.
(32) Yamada, R.; Ara, M.; Tada, H. *Chem. Lett.* **2007**, *33*, 492−493.
(33) Sung, M. M.; Kluth, G. J.; Yauw, O. W.; Maboudian, R. *Langmuir* **1997**, *13*, 6164−6168.
(34) Faucheux, A.; Gouget-Laemmel, A. C. G.; Allongue, P.; Henry, de Villeneuve, C.; Ozanam, F.; Chazalviel, J.-N. *Langmuir* **2007**, *23*, 1326−1332.